Influence of ageing on the structure and phosphate adsorption capacity of dewatered alum sludge

Y. Yang, Y.Q. Zhao *, P. Kearney

Centre for Water Resources Research, School of Architecture, Landscape and Civil Engineering, Newstead Building, University College Dublin, Belfield, Dublin 4, Ireland

ARTICLE INFO

ABSTRACT

In line with the increasing studies on the beneficial reuse of alum sludge from a "waste" into useful raw material, this paper reports an in-depth investigation of the effects of ageing time on the structure and the phosphate adsorption capacity of a dewatered alum sludge obtained from a local drinking water treatment plant in Ireland. During the ageing period from 0 day to up to 18 months, the adsorption capacity of the sludge varied from 21.4 to 23.9 mg P g^{-1} sludge at pH 4.3, 14.3 to 14.9 mg P g^{-1} sludge at pH 7.0 and 0.9 to 1.1 mg P g^{-1} sludge at pH 9.0, respectively, indicating marginal effect of ageing time on such sludge's ability to adsorb phosphate. This result seems in conflict with other studies reported in the literature. To reveal such, series of investigations including physicochemical characterization, morphological structure, Brunauer–Emmett–Teller (BET) surface area and porous structure of the aged sludge were carried out. All the results conclusively show that ageing time has an insignificant effect on the structure and properties of the dewatered alum sludge and therefore, the phosphate adsorption capacity of the alum sludge shows insignificant change during the ageing process.

1. Introduction

Phosphorus (P) is an essential nutrient for the growth of aqueous plants and is also a principal element to cause eutrophication in the water environment. Generally, the biological phosphorus removal (BPR) process and/or chemical precipitation are used in the removal of P from wastewater. In chemical removal, lime and metal salts, such as aluminium, iron and magnesium salts are used for this purpose [1]. However, this can increase the operational costs and/or sludge production, thus hindering its widespread use. Therefore, other cost effective treatment methods and materials are being investigated. Alum sludge is an inevitable by-product of the production of drinking water when aluminium salt is added as a coagulant. In Ireland, as in most other countries worldwide, alum sludge is historically reviewed as 100% "waste" and disposed of in landfill sites. However, following sustainability principles, there is a progressive drive towards alum sludge reuse as a beneficial material. In particular, previous work done by investigators including the authors showed that alum sludge has a considerable adsorption capacity and can be utilized as a low-cost adsorbent for P immobilization from wastewaters and contaminated soils [2–9].

Factors to influence P-adsorption capacity of alum sludge are mainly derived from two catalogues. One is from the sources/processes of the sludge to be formed, such as source water quality, dose of alum salt and other chemicals, water treatment process etc. [3] and the other is from the P-sorption testing conditions, such as particle size, equilibrium time, initial P concentration [2,5,10,11]. Furthermore, ageing time of the sludge appears to affect the P sorption capacity as well. DeWolfe [3] reported that the ability of alum sludge to bind P is likely due to a multitude of factors including the age of the sludge. It is claimed that the old/aged alum sludge is likely to be less reactive due to mineralization of aluminium. Compared with aluminium hydroxides, alum sludge may have different but similar characteristics in structure and P-adsorption mechanism. Amorphous aluminium hydroxide, which is thermodynamically metastable, can be transformed to thermodynamically stable phases with increasing ageing time, pH and temperature [12]. The path of structural transformation could be different with various mobility of ions that are related to the water content [13]. In the ageing process under aqueous condition, it was reported that the Brunauer–Emmett–Teller (BET) surface area of aluminium hydroxide floc formed from aluminium sulphate addition to lake waters, was decreased from 72 $m^2\,g^{-1}$ (at 4 days of ageing) to 38 $m^2\,g^{-1}$ (at 120 days) and was accompanied by the transformation of amorphous Al(OH)$_3$ to gibbsite which increases the crystallinity of the aluminium hydroxide floc [14]. The significant decrease of the surface area of the floc over ageing time is

* Corresponding author. Tel.: +353 1 7163215; fax: +353 1 7163297.
E-mail address: yaqian.zhao@ucd.ie (Y.Q. Zhao).

believed to be related to the structural transformation [14–16]. The P-adsorption capacity of aluminium hydroxide floc aged for 6 months was about 50% lower than the fresh floc; this is likely due to the alterability of the structural transformations and the reactivity of P-adsorption [14].

During the ageing process under dry conditions, however, structural transformation does occur, but at lower rates since the ion mobility is restricted [13]. It was reported that alum sludge showed no significant change in the structure, adsorption sites and P-adsorption capacity despite ageing of the sludge in the laboratory for approximately 5 years [17]. Interestingly, aluminium hydroxide sample prepared at 70 °C showed a significant decrease in surface area and micropore volume within the first month of the ageing process [6]. Although the sludge samples were collected from different locations and the experimental conditions might be different, the conflicting results emphasize the need for a more detailed and in-depth study into the effect of the ageing time on structure and the P capacity of the alum sludge. This forms the basis of the present study.

However, whether ageing affects the P-adsorption capacity of alum sludge or not will depend on the influence of the ageing time on the structure and surface properties of alum sludge. Therefore, the objectives of this study were to (1) identify the effect of ageing time on P-adsorption capacity of dewatered alum sludge and (2) characterize the structure and the surface properties of alum sludge during the ageing process of up to 18 months.

2. Materials and methods

2.1. Source of dewatered alum sludge and sample preparation

Dewatered alum sludge cakes were collected from an industrial filter press of the sludge dewatering unit of the Ballymore Eustace Water Treatment Plant, Co. Kildare, Ireland. The plant produces about 230,000–275,000 $m^3 d^{-1}$ of potable water for Dublin city. The raw water with a mean colour of 105 Hazen units flows through a series of tunnels under gravity from the Poulaphuca reservoir, 1.5 km away from the plant. Aluminium sulphate is used as the primary chemical coagulant at a dose of 42–60 $mg L^{-1}$. After collection, the sludge cakes (moisture content 72–75%) were stored at room temperature in a well-covered container for a period of up to 18 months, during which the samples of sludge stored for 0 day (fresh alum sludge), 6, 12, and 18 months were subjected to various tests for their chemical properties, P-adsorption capacities and structures. It should be pointed out that, to eliminate the affect of air-drying process on the moisture content of the sludge, the sludge was stored in a well-covered environment, causing the anaerobic condition of the sludge during ageing process. However, the potential effects of anaerobic condition on the structure and properties of alum sludge were not considered in the current study. Before tests at each specific ageing time, the sludge samples were taken from the storage and air-dried at room temperature for 1 week. The sludge was then ground and sieved to provide the test adsorbent with diameter <0.063 mm.

2.2. Chemical characterization of the alum sludge

The prepared alum sludge samples at each ageing time were dried in an oven at 103 ± 2 °C for 72 h to determine the moisture content. The 103 ± 2 °C dried samples were weighed and digested using the standard method of nitric acid digestion (3030 E) [18]. Thereafter, the chemical composition of the samples was examined using inductively coupled plasma-optical emission spectrum (ICP-AES, IRIS Intrepid II XSP, Thermo Elemental, Franklin, Mas-

sachusetts, USA), ion chromatography (DX-120, Dionex, Sunnyvale, California, USA) and total organic carbon (TOC)-V$_{CSH}$ (Shimadzu, Tokyo, Japan).

2.3. Adsorption capacity

Adsorption capacity of the sludge sample at each specific ageing period was determined using batch tests. Different masses of the alum sludge ranging from 0.2 to 20.0 $g L^{-1}$ were prehydrolyzed in a pH controlled distilled water (pH 4.3–9) for 48 h. Thereafter, standard aliquots of the P stock solution, which were prepared by dissolving pre-weighed potassium dihydrogen phosphate (KH_2PO_4) in distilled water, were then introduced, giving a resultant initial P concentration of 100 $mg P L^{-1}$, and alum sludge content ranged from 0.1 to 10.0 $g L^{-1}$. The mixtures were then mechanically agitated to enhance adsorption over a 48 h equilibration period that was pre-determined in the previous study [4]. During this period, the solution was adjusted to the required pH (ranged from 4.3 to 9.0) using sulphuric acid (0.01 M) and sodium hydroxide (0.1 M). After adsorption, equilibrated samples were filtered using 0.45 μm millipore filter paper (Millipore, Billerica, Massachusetts, USA) and analysed for P concentration using the stannous chloride method (4500-P D) [18]. The equilibrium adsorption capacities were calculated from a linearized form of the Langmuir adsorption isotherm [19].

$$\frac{C_e}{q} = \frac{1}{Q_0}C_e + \frac{1}{Q_0 b} \tag{1}$$

where q is the mass of P adsorbed per unit mass of sludge($mg P g^{-1}$ sludge); C_e is the equilibrium concentration of phosphate in the suspension ($mg P L^{-1}$); Q_0 is the maximum adsorption capacity ($mg P g^{-1}$ sludge); b is the constant related to the energy of the adsorption–desorption process with unit of inverse of concentration C_e. By plotting C_e vs. C_e/q, a straight line with slope $1/Q_0$ is obtained and the Q_0 can be calculated.

2.4. Morphological and structural characterization

2.4.1. Morphological structure and functional group characterization

The morphology of each sludge sample at different ageing times was examined by scanning electron microscope (SEM, JSM-6700F, Japan Electron Optics Laboratory, Tokyo, Japan) and X-ray powder diffraction (XRD, D/max-3C, Rigaku, Tokyo, Japan). The functional group of the sludge was also examined by attenuated total reflectance Fourier transform infrared (ATR-FTIR) (EQUINOX-55, Bruker, Ettingen, Germany).

2.4.2. BET surface area and pore structure

Low temperature nitrogen adsorption–desorption isotherms: To determine the surface area and the pore characteristics of the alum sludge, the prepared sample (air-dried, particle diameter <0.063 mm) was outgassed at 250 ± 5 °C for 3 h until the relative pressure (p/p^0) was less than 10^{-6}. Thereafter, low temperature nitrogen adsorption–desorption isotherms at 77.4 ± 0.1 K were conducted using a surface area and pore size analyzers (SA3100, Beckman Coulter, Fullerton, California, USA).

BET surface area: The BET surface area was calculated by fitting the nitrogen adsorption isotherm data to the BET model [20] (see Eqs. (2)–(4))

$$\frac{p/p^0}{n(1-p/p^0)} = \frac{1}{n_m c} + \frac{c-1}{n_m c}\left(\frac{p}{p^0}\right) \tag{2}$$

$$A_{BET} = 4.35 n_m, \quad n_m = \frac{1}{s+i} \tag{3}$$

$$c = \frac{s}{i} + 1 \tag{4}$$

where p/p^0 is the relative pressure; n is the volume of the gas adsorbed at p/p^0 (mL(STP)g^{-1}); n_m is the monolayer adsorption capacity (mL(STP)g^{-1}); c is the BET constant which is approximately equal to $e^{(E_l - E_L)/RT}$ (E_l is the heat of adsorption of the gas in the first adsorbed layer, and E_L is the heat of liquefaction of the gas); A_{BET} is the specific surface area calculated from BET model.

Mesopore pore size distribution: The mesopore size distribution was obtained from the desorption branch of the low temperature nitrogen isotherm using the method of Pierce [21]. The hysteresis loop range used for pore size distribution was from $p/p^0 = 0.948$ to 0.445 (fresh sample), 0.956 to 0.434 (6 months old sample), 0.948 to 0.465 (12 months old sample), and 0.957 to 0.45 (18 months old sample), respectively.

Micropore and micropore surface area: The micropore identification was carried out and the micropore surface areas of the alum sludges were examined using the t-plot. t-Plot is a plot of the isotherm with the statistical thickness of the film (t). Fitting the linearized Harkins–Jura (HJ) model (see Eq. (5)) to the experimental data, the constants a and b can be determined [22]. Thereafter, t is determined by using the HJ equation (see Eq. (6)). In the range $t \leq 3.54$ Å, the slope of the straight line can be used to obtain the surface area (indicated as $A_{t,HJ}$) and this can be used as criterion to test the correctness of the pore type identification model. In the range $t > 3.54$ Å, the slope of the straight line gives the mesopore surface area (indicated as $A_{t,HJ,Meso}$) of the adsorbent. The difference between $A_{t,HJ}$ and $A_{t,HJ,Meso}$, gives the surface area contributed by micropore (if the micropore is present) [23,24].

$$\log\left(\frac{p}{p^0}\right) = b - \frac{a}{(n/n_m)^2} \tag{5}$$

$$t = 3.54 \left[\frac{a}{b - \log(p/p^0)}\right]^{1/2} \text{ (Å)} \tag{6}$$

where 3.54 Å corresponds to the thickness of the nitrogen layer [25].

3. Results

3.1. Chemical composition of the alum sludge

The quantitative chemical composition of the alum sludge at different ageing times is given in Table 1. The dominant component in all the sludge samples is aluminium (as Al_2O_3) with approximately 424.3, 430.4, 418.9 and 436.7 mg g^{-1} sludge in 0 day, 6, 12 and 18 months' storage, respectively. In spite of some scatter, the insignificant change of the aluminium content (in the range from -1.3% to 2.9%) during the ageing period studied was observed. The moisture content of the samples of 0 day, 6, 12 and 18 months' ageing time is 34.6%, 24.7%, 25.3% and 24.6%, respectively. This shows similarity in free-water content of the sludges under different ageing times, especially after 6 months. The mass loss at 500 °C is due to the loss of volatile organic matter and also part of the structural hydroxyl ion. At 1000 °C, the mass loss is caused by the loss of structural hydroxyl ion. Overall, the striking feature of the data in Table 1 lies in the insignificant difference in the chemical characteristics of the sludge throughout the 18 months ageing period, which shows considerable stability in its chemical characteristics.

3.2. Effect of ageing time on P-adsorption capacity

The effect of the ageing time on P-adsorption capacity of the alum sludge at different pH conditions is shown in Fig. 1. The maximum adsorption capacity, Q_0, obtained using Langmuir isotherm, in
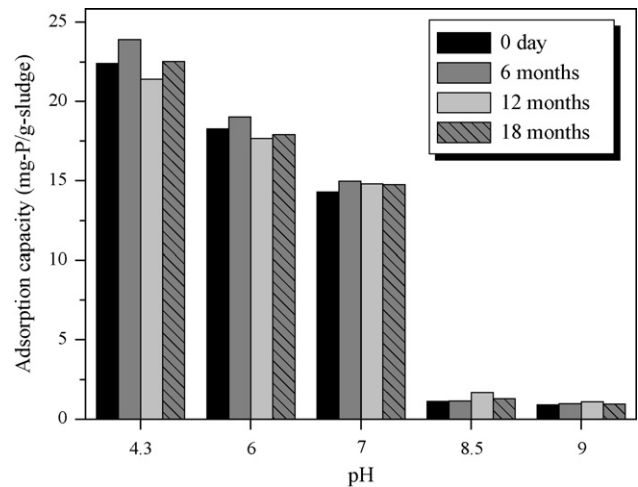

Fig. 1. P-adsorption capacity of the alum sludge at different ageing times and pH condition.

18 months ageing varied 21.4–23.9 (at pH 4.3), 17.7–19.1 (at pH 6.0), 14.3–14.9 (at pH 7.0), 1.1–1.7 (at pH 8.5) and 0.9–1.1 mg P g^{-1} sludge (at pH 9.0). These results clearly show that the adsorption capacity of the alum sludge decreases with increasing pH, which has been examined in our earlier studies [4,5]. It is however more important to note that the ageing seems not to considerably affect the P-adsorption capacity of the alum sludge since the change <5% in maximum adsorption capacity during the ageing process was statistically obtained.

3.3. Effect of ageing time on sludge structural characteristics

3.3.1. Solid-phase structural transformation

Fig. 2 illustrates the X-ray diffraction patterns of the fresh and aged sludges. It can be seen clearly that the fresh and aged sludges exhibit quite similar XRD characteristics. There is no considerable crystalline-aluminium related XRD peak observed. This indicates that crystallization (a process of transformation of amorphous form
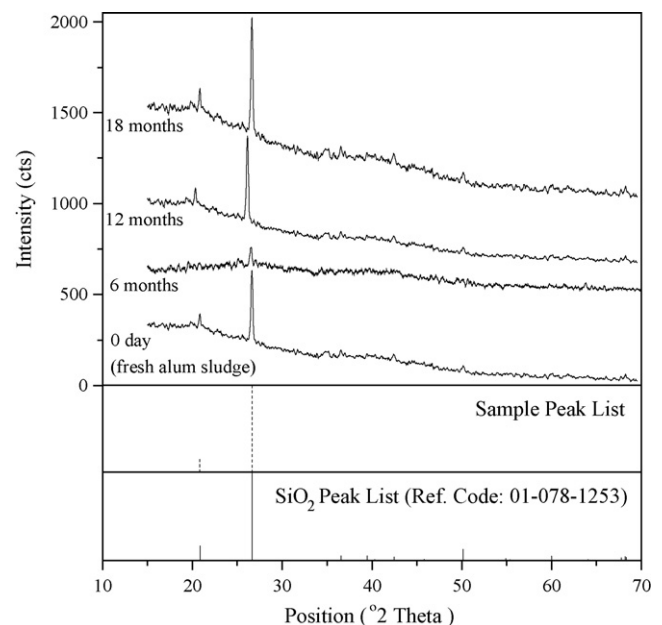

Fig. 2. X-ray diffraction patterns of alum sludge at various ageing times.
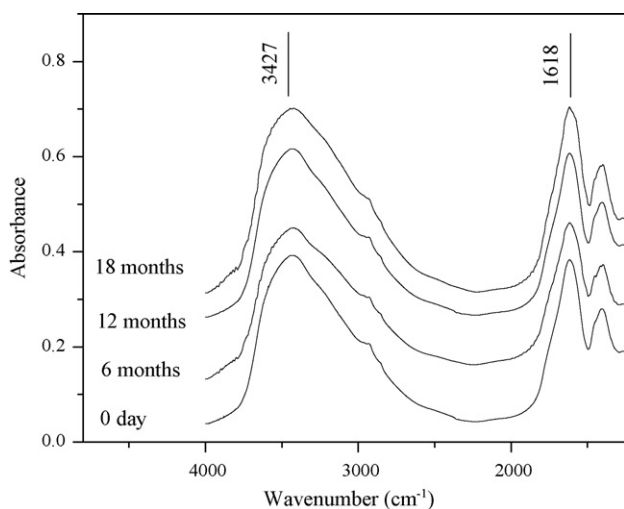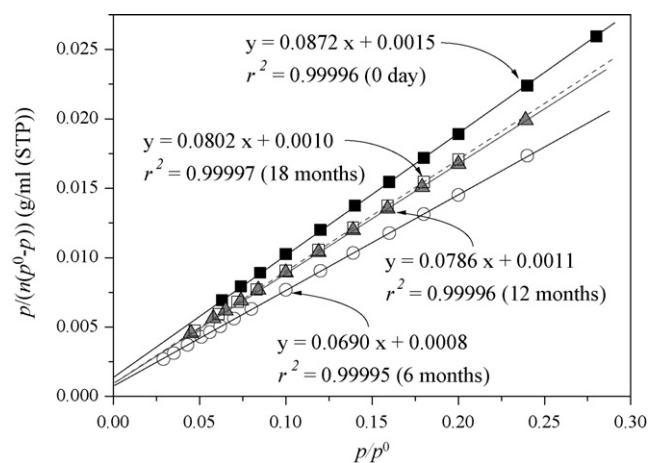
Table 1
The chemical components of the fresh alum sludge (ageing time: 0 day) and the aged alum sludge (ageing time: 6, 12 and 18 months)

Chemical composition	Unit	Amount (mean ± S.D.)			
		0 day	6 months	12 months	18 months
Moisture content	%	34.59 ± 1.87	24.73 ± 0.52	25.25 ± 1.0	24.58 ± 1.59
Aluminium (as Al_2O_3)	$mg\,g^{-1}$ sludge	424.3 ± 2.97	430.4 ± 8.63	418.9 ± 1.44	436.7 ± 1.01
Iron (as Fe_2O_3)	$mg\,g^{-1}$ sludge	8.86 ± 0.67	11.00 ± 0.85	9.01 ± 1.30	12.2 ± 0.36
Calcium (as CaO)	$mg\,g^{-1}$ sludge	8.77 ± 0.61	11.46 ± 0.51	8.87 ± 0.25	8.32 ± 0.49
Magnesium (as MgO)	$mg\,g^{-1}$ sludge	4.11 ± 0.69	7.34 ± 0.31	6.75 ± 0.27	5.77 ± 0.33
Humic acid (as TOC)	$mg\,g^{-1}$ sludge	145.1 ± 2.91	101.6 ± 4.17	156.1 ± 1.47	137.3 ± 1.83
Cl^-	$mg\,g^{-1}$ sludge	15.89 ± 0.09	15.73 ± 0.47	16.31 ± 0.17	16.41 ± 0.37
$SO_4{}^{2-}$	$mg\,g^{-1}$ sludge	9.73 ± 0.35	8.57 ± 0.16	8.72 ± 0.19	9.34 ± 0.23
Silicon oxide (as SiO_2)	$mg\,g^{-1}$ sludge	27.67 ± 1.90	13.17 ± 0.83	24.01 ± 1.67	27.76 ± 0.94
Mass loss at 500 °C	%	54.96 ± 0.12	50.29 ± 0.43	53.59 ± 0.17	54.85 ± 0.08
Mass loss at 1000 °C	%	0.23 ± 0.01	0.24 ± 0.03	0.24 ± 0.02	0.24 ± 0.02

to crystalline) did not occur during the ageing process. In contrast, the XRD pattern elucidates the amorphous structure of the alum sludge. The peak in Fig. 2 is identifiable crystalline solid of silicon oxide (SiO_2), which can be identified by the powder diffraction file (PDF).

3.3.2. Functional groups on the surface of the aged sludges

Fig. 3 shows the ATR-FTIR spectra of the alum sludge at different ageing times. The comparison of ATR-FTIR spectra can reveal the transformation (if any) of the hydroxyl group (–OH) on surface of alum sludge at different ageing times. The surface hydroxyl group is essentially related to the adsorption capacity of the alum sludge due to the fact that the functional group plays a dominant role in the ligand exchange mechanism of the P-adsorption onto the surface of alum sludge [5]. The OH vibration detected in the ATR-FTIR spectra of the sludge can reveal any transformation of the OH group on the alum sludge. The bonded OH stretching vibration can be detected at ca. 3400 (3600–3200) cm^{-1} (antisymmetric and symmetric OH stretching mode) and 1625 (1650–1600) cm^{-1} (HOH bending mode) [26,27]. From Fig. 3, it can be seen that the spectrum is characterized by a broad peak which is due to functional group vibration at 3427 and 1618 cm^{-1} for all the sludge samples, irrespective of their ageing time. The main adsorption band in the spectrum of the alum sludge appeared at 3427 cm^{-1} and this can be identified as the OH group due to its vibration [27,28], while the absorption at 1618 cm^{-1} can be potentially linked to the bonded OH and/or organic functional group (i.e. C=C, C=N) [29,30]. Notwithstanding the ageing time, the intensity of the OH and/or C=C and C=N vibra-

Fig. 4. BET plots of low temperature nitrogen adsorption isotherm of the fresh alum sludge (ageing time: 0 day) and the aged alum sludges (ageing time: 6, 12 and 18 months).

tions did not change. The similar characteristics of the ATR-FTIR of the different aged sludge samples, as shown in Fig. 3, lead to the conclusion that there was no transformation of functional groups during the ageing process. This implies that the ageing time did not affect any change of the functional group (–OH and/or humic substances) on the surface of the alum sludge.

3.3.3. BET surface area of the aged sludges

The BET plots of the aged alum sludges, which were obtained by applying Eq. (1) to experimental data, are presented in Fig. 4. The n_m, BET c-constant and surface area (A_{BET}) can be calculated from the BET model and the results are shown in Table 2. The A_{BET} of the alum sludge at different ageing times is respectively 49.03 $m^2\,g^{-1}$ sludge (0 day, fresh alum sludge), 62.33 $m^2\,g^{-1}$ sludge (6 months), 54.60 $m^2\,g^{-1}$ sludge (12 months), and 53.54 $m^2\,g^{-1}$ sludge (18 months). This indicates that the surface area of alum sludge was not decreased with the ageing time. In contrast, a considerable increase of the surface area at 6 months

Fig. 3. ATR-FTIR spectra of alum sludge samples with different ageing times.

Table 2
Results of BET plot using nitrogen adsorption isotherm of the fresh alum sludge (ageing time: 0 day) and the aged alum sludges (ageing time: 6, 12 and 18 months)

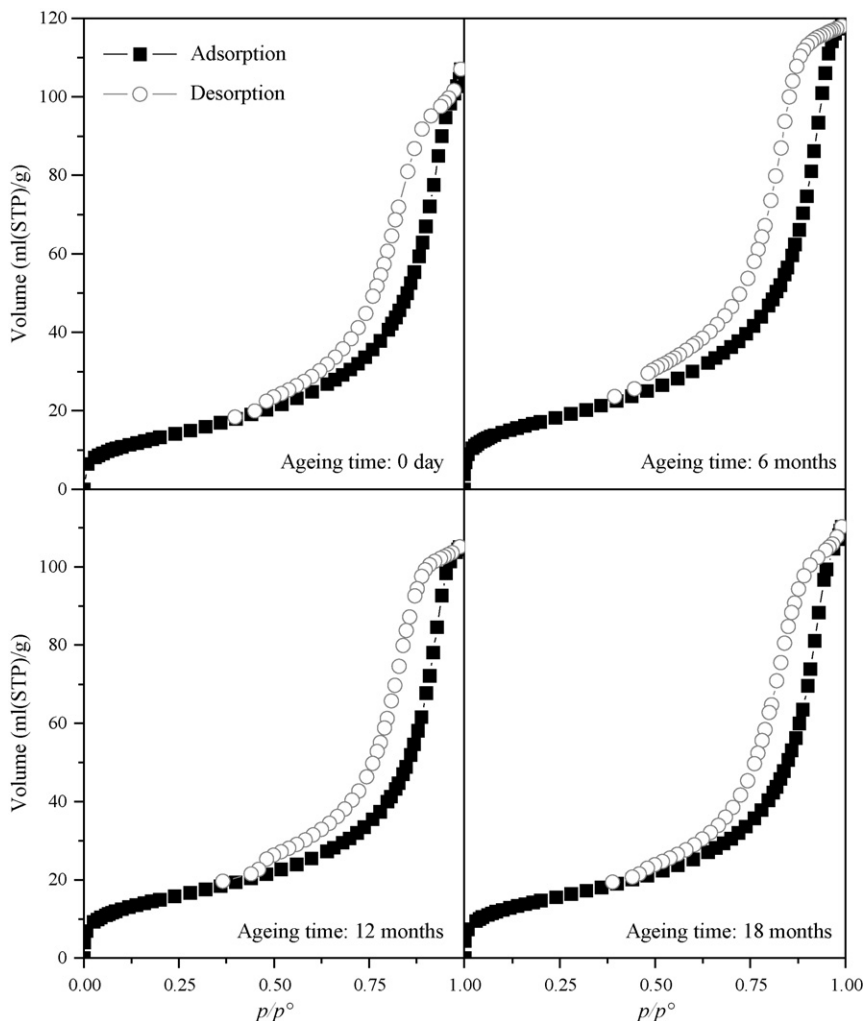| Ageing time	p/p^0 range	n_m ($mL(STP)\,g^{-1}$)	BET c -constants	A_{BET} ($m^2\,g^{-1}$)	r^2
0 day	0.063–0.280	11.27	59.09	49.03	0.99996
6 months	0.029–0.240	14.33	92.58	62.33	0.99995
12 months	0.045–0.239	12.55	75.84	54.60	0.99996
18 months	0.047–0.200	12.31	79.63	53.54	0.99997

Fig. 5. Nitrogen adsorption–desorption isotherms at 77.4 K for different ageing times of alum sludges.

was observed. Although there was some difference in the surface area of the samples, this is rather caused by sample differences (see Table 1) and not particularly due to the effect of the ageing time. It is also noted in Table 2 that the value of BET c-constant for the different alum sludge samples is approximately the same, while the monolayer adsorption capacity (n_m) did not differ significantly. This indicates that there was no significant change in surface properties of alum in spite of their different ageing times.

3.3.4. Porous structure of the aged alum sludges

The nitrogen adsorption–desorption isotherm is presented in Fig. 5. From the adsorption branch, the isotherm of the alum sludge represents Type IV according to the Brunauer–Deming–Deming–Teller (BDDT) classification [31], while the desorption branch exhibits a wide hysteresis loop. The hysteresis loop refers to a phenomenon in which the desorption isotherm curve does not coincide with the adsorption isotherm curve. This is caused by the fact that the nitrogen released during the desorption process is always less than the amount of nitrogen adsorbed during the adsorption over the high relative pressure range, a phenomenon caused by the condensation in the pores or capillaries. The hysteresis loop occurred over the entirely high relative pressure range, i.e. at $p/p^0 = 0.445$–0.991 (0 day, fresh alum sludge); 0.434–0.99 (6 months); 0.465–0.989 (12 months) and 0.45–0.99 (18 months), which represents the capillary condensa-

tion. The very similar trends of the hysteresis loops of the different samples clearly indicate the unchanged porous structure of the sludge during the ageing time tested.

3.4. SEM observation of the aged alum sludges

Fig. 6(a–d) shows the SEM images of the alum sludge at different ageing times. The presence of the cylindrical-like shape, mesosize pores (which are several tens of nanometres in diameter) in the alum sludges can be observed from Fig. 6. More importantly, from the comparison of the SEM images, the very similar amorphous structures of the sludges can be observed despite their different ageing times. Both the morphological structure, pore size and the pore shape remain unchanged during the ageing process. This further proves the non-structural transformation during the ageing process, although the SEM provides a qualitative description.

4. Discussion

4.1. Effect of ageing time on structural transformation

In considering the use of alum sludge as a low-cost adsorbent for P immobilization, the need for detailed investigation of ageing effect on its P-adsorption ability is a crucial necessity in both academic and practical respects. It is believed that the adsorp-
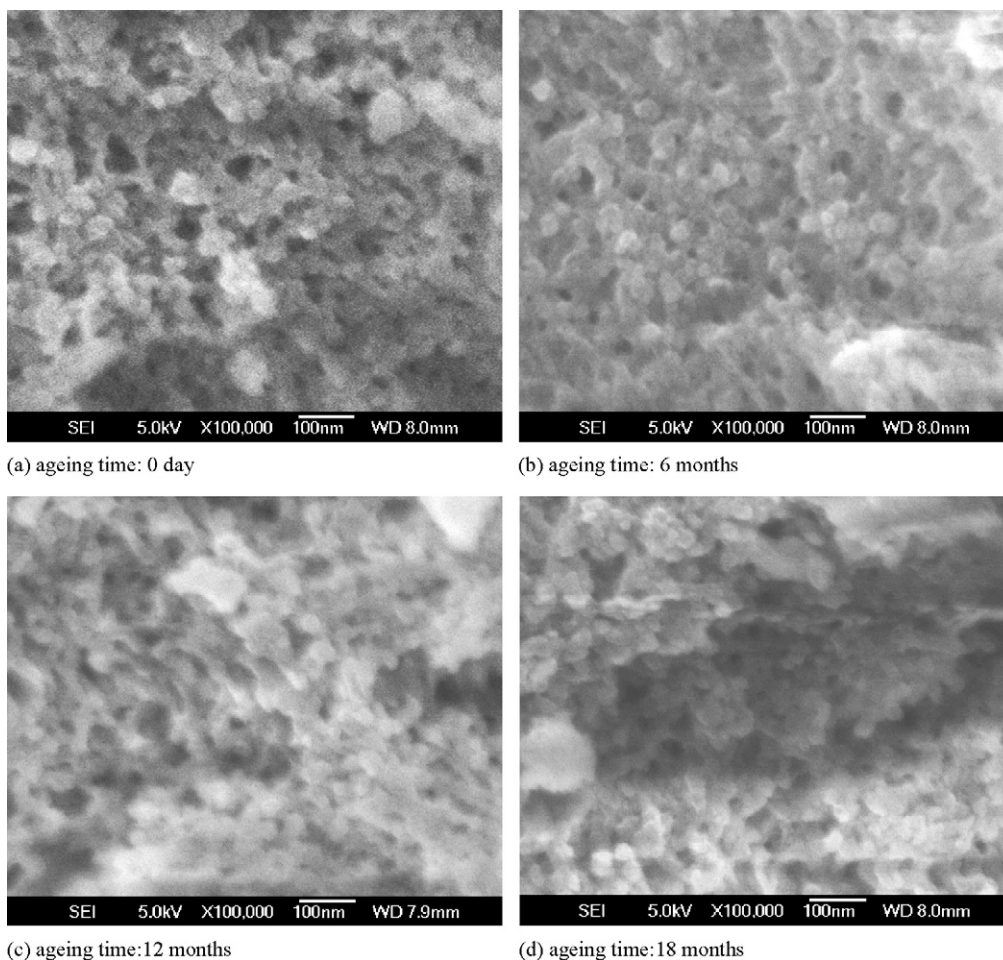
(a) ageing time: 0 day

(b) ageing time: 6 months

(c) ageing time:12 months

(d) ageing time:18 months

Fig. 6. SEM images of the fresh alum sludge (ageing time: 0 day) and the aged alum sludges (ageing time: 6, 12 and 18 months).

tion capacity of alum sludge depends on the chemical nature of the sludge. Any changes of its chemical characteristics and related structure and surface properties during the sludge ageing process will be useful to identify and understand the change (if any) of its P-adsorption ability. Current evidence from literature seems to reveal some conflict regarding this. In an evaluation of the influence of ageing time on P-adsorption capacity of aluminium hydroxide floc, it was shown that approximately 20% of the floc had transformed to gibbsite after 20 days and over 70% was transformed in 180 days ageing time [14]. More recently, Georgantas and Grigoropoulou [32] provided the evidence on XRD monitoring of aluminium hydroxide during ageing. It has been demonstrated that the characteristic diffraction band of gibbsite appeared in the second month of ageing and this diffraction band becomes sharper with time. Accordingly, the P sorption capacity was reported to decrease with the structural transformation. One possible reason could be the decrease of the non-structural –OH, due to its transformation into the structural –OH during the ageing process of aluminium hydroxide. The result in the decrease of available ligand exchangeable ion subsequently leads to the decrease in P-adsorption capacity [16,33]. It is important to note that the above claims of the structural transformation of the aluminium hydroxide (flocs) were based on the ageing in aqueous condition. However, in an artificial ageing process (referring to both thermal and wet and dry incubation) of a relative dry condition of alum sludge amended soils, it was reported that P would remain immobilized and there was no release in the long term [34]. Also in dry ageing condition, this study revealed that the

amorphous structure of the alum sludge (see Fig. 2) did not change into the thermodynamically stable structure (crystalline) during 18 months. The cause of this is likely due to the fact that such structural changes are kinetically very slow especially in dry conditions [35], although they are certainly thermodynamically possible. In addition, the presence of organic acid [36] and/or ionic strength may slow this process [16,37]. Consequently, the unchanged surface structure and functional group of alum sludge can be suggested as reasons for the insignificantly changed P-adsorption capacity (see Fig. 1).

4.2. Effect of ageing time on surface area

In a study of P-adsorption on alum hydrolysis products, it was reported that the transformation of amorphous aluminium hydroxide to crystalline form was accompanied by a decrease of surface area over the ageing time [38]. This may affect the reactivity of the aluminium hydrolysis products and the availability of the surface area that are crucial for P-adsorption. As a result, the adsorption capacity was decreased during the ageing period [14,36]. However, the examination on the surface area of the aged sludges in this study (Fig. 4) provides hard evidences to support the fact of insignificant change of surface area during the ageing process. It is believed that the surface area must be sufficient enough to accommodate the P molecules located on the surface of the alum sludge. This is particularly important as most of the surface area is located in the interior of the alum sludge particle. Therefore, any significant decrease in
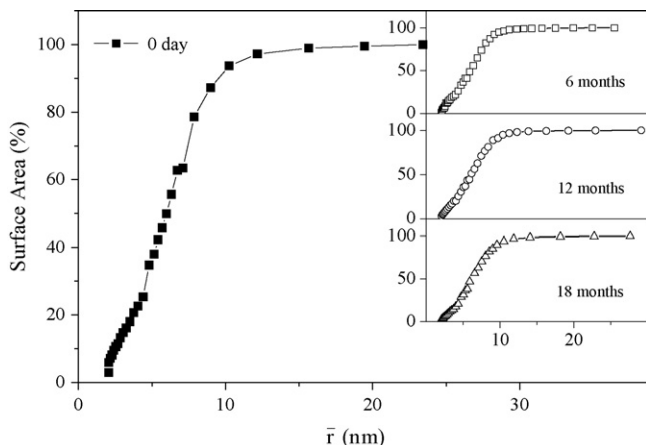
Fig. 7. Mesopore surface area–pore size distribution of the fresh alum sludge (ageing time: 0 day) and the aged alum sludges (ageing time: 6, 12 and 18 months).

the surface area of alum sludge during the ageing period can reduce the adsorption capacity. Therefore, the unchanged surface area can be attributed as reasons for the unchanged adsorption capacity (see Fig. 1).

4.3. Effect of ageing time on pore size distribution and pore type

4.3.1. Effect of ageing time on pore size distribution

The pore type and the pore size of alum sludge are crucial for P-adsorption since alum sludge should provide enough pathway through which the adsorbate molecules can gain access into the interior of the alum sludge particle. Therefore, any significant change in pore type and the pore size during the ageing process can result in the change of the sludge adsorption capacity.

A characteristic feature of mesopore solid is that its adsorption isotherm represents Type IV with a hysteresis loop [39]. The Type IV adsorption isotherm and the hysteresis loop in the adsorption–desorption isotherm of the current study indicate clearly the existence of the mesoporous structure of the alum sludge (Fig. 5). From the SEM images, the presence of cylindrical-like mesopore can be qualitatively seen in various aged sludge samples (see Fig. 6).

To further characterize the structural change in terms of pore size distribution during the ageing process, a comparative quantitative method is applied to reveal the porous structure and its change in more detail. The mesopore size distribution based on surface area is shown in Fig. 7. The main feature of this illustration is a very similar characterization in pore size distribution with different ageing times of the sludge. Fifty percent of the surface area of the ageing sludges is contributed by pores with sizes less than 5.98 nm (0 day), 6.13 nm (6 months), 6.10 nm (12 months) and 6.17 nm (18 months), while ninety percent of surface area is contributed by pores of size less than 9.67 nm (0 day), 9.01 nm (6 months), 9.39 nm (12 months) and 9.60 nm (18 months). The pores with sizes larger than 20 nm only contributed insignificant amount to the surface area. The slight difference in pore size distribution between the ageing sludges is most likely due to sample differences rather than the ageing time. Accordingly, the unchanged surface area can be attributed as reason for the unchanged adsorption capacity (see Fig. 1).

4.3.2. Effect of ageing time on pore type

In addition, to reveal the entire porous structure and characteristics of the alum sludge, t-plot can be employed to reveal both qualitative and quantitative information about the micropore [23]. For the non-porous solid, the t-plot is a straight line through the
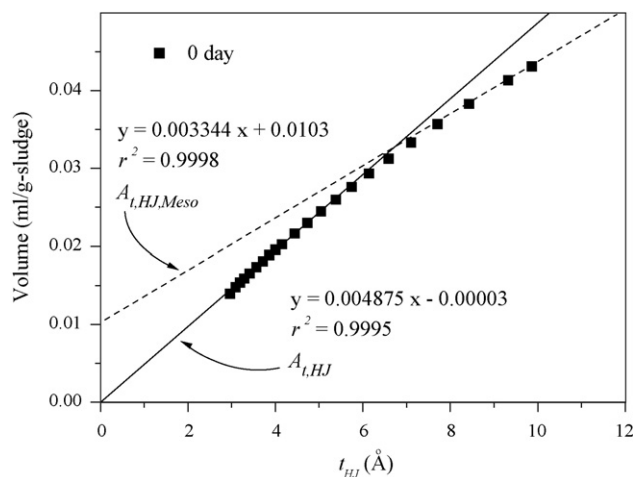

Fig. 8. t-Plot of the fresh alum sludge (ageing time: 0 day) (using HJ model and HJ t-equation).

entire multilayer adsorption range and the straight line through the origin. For the porous solid, the straight line can be obtained in the low pressure range. The difference between the t-plot straight line and the t-curve can be used to characterize the presence or otherwise of a certain type of pore [23,40,41]. The t-curve, as shown in Fig. 8, exhibits a downward deviation from the straight line. This is observable in the fresh alum sludge (ageing time: 0 day) only.

The upward deviation of t-curve from the straight line, as shown in Fig. 9, suggests that there are no micropores in the 6, 12 and 18 months old samples. From the intercept of the t-plot, the presence or otherwise of the micropores can be quantitatively and qualitatively determined. From the comparison of the porous structure based on the t-plot, it can be noted that the only porous structural change during the ageing process is the disappearance of the micropores in the alum sludge. The micropore surface area in the fresh sample (ageing time: 0 day) is 15.31 m^2/g sludge and this represents 31.41% of the entire surface area (see Table 3). The comparison of the surface area obtained through the BET model (A_{BET}) (see Table 2) and the t_{HJ}-plot ($A_{t,HJ}$) (see Table 3) shows that the $A_{t,HJ}$ is 0.57% (0 day), 0.87% (6 months), 2.31% (12 months) and 2.07% (18 months) lower than A_{BET}. The good agreement between A_{BET} and $A_{t,HJ}$ shows the validity of using HJ model and HJ t-equation to characterize the pore type of the aged alum sludges.
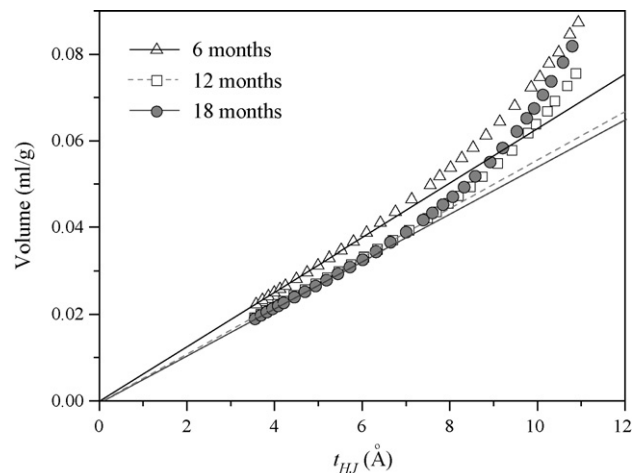

Fig. 9. t-Plot of 6, 12 and 18 months aged alum sludge (using HJ model and HJ t-equation).

Table 3
Harkins–Jura model constants and t_{HJ}-plot results of the fresh alum sludge (ageing time: 0 day) and the aged alum sludges (ageing time: 6, 12 and 18 months)

	HJ model			$A_{t,HJ}$			Mesopore			Micropore surface area (m^2 g^{-1})
	a	b	r^2	p/p^0 range	t_{HJ} range (Å)	$A_{t,HJ}$ (m^2 g^{-1})	p/p^0 range	t_{HJ} range (Å)	$A_{t,HJ,Meso}$ (m^2 g^{-1})	
0 day	0.864	−0.068	0.9996	0.05–0.100	2.96–3.41	48.75	0.32–0.6	5.04–8.40	33.44	15.31
6 months	1.065	0.040	0.9999	0.051–0.080	3.16–3.42	61.79	0.10–0.32	3.58–4.99	62.97	0
12 months	1.041	0.039	0.9998	0.045–0.084	3.07–3.42	53.34	0.10–0.32	3.54–4.94	55.59	0
18 months	1.056	0.048	0.9999	0.039–0.083	3.03–3.42	52.43	0.10–0.32	3.54–4.93	54.45	0

Overall, the approaches used to reveal the chemical composition, morphological structure, surface functional group, surface area, pore type and pore distribution, which are believed to be highly relevant in affecting the adsorption ability of alum sludge, support the idea of inconsiderable change in the P-adsorption capacity of dewatered alum sludge over ageing time. The adsorption capacity of the alum sludge, being 'ageing time-independent', is almost definitely due to its 'unchanged' chemical and structural characteristics with ageing time.

5. Conclusions

The results of this study provide insight and concrete evidence to demonstrate the stability of the structure and surface characteristics of the alum sludge over time. It further provides basis to the unexpected change in P-adsorption capacity of alum sludge over time. Despite the inherent variability of the alum sludge samples, the results of SEM, XRD, ATR-FTIR, nitrogen adsorption–desorption isotherm, surface area, pore area and pore size distribution indicated that the ageing time has no significant effects on the structure and surface characteristics. The major conclusions of this study are:

- Results of SEM and XRD show that solid-phase transformation did not occur during the 18 months ageing process. Although the alum sludge has an amorphous structure, which is thermodynamically metastable, there was no morphological structural transformation observed in the aged sludge. This indicates that the influence of ageing time on the structure and surface properties of alum sludge is different from that of pure aluminium hydrolysis products because the two solid phases have totally different chemical characteristics and composition. In addition, transformation of the aged alum sludge into more stable forms is not observed and this is adduced to be a combination of the kinetic behaviour, environmental conditions and/or the presence of other inhibiting materials.
- The ATR-FTIR result indicates that the functional group on the surface of the alum sludge did not change over the ageing time.
- The BET surface of the aged sludges did not decrease during the ageing process. The type of low temperature nitrogen adsorption–desorption isotherm and the SEM images indicate that the alum sludge is structurally mesoporous. The t_{HJ}-plot results illustrate that the fresh alum sludge (ageing time: 0 day) contains micropores while for the 6, 12 and 18 months aged sludge there was no micropore being observed. This is likely thought to be due to the extended ageing time which may control the entirely mesoporous structure of the alum sludge. Results of the mesopore size distributions also show that the alum sludge samples have a similar size distribution with a narrow pore size distribution. There was no significant change over the ageing time.
- The findings of the current investigation are vital for two main reasons: (1) Aside from revealing the in-depth phenomena of the ageing process of alum sludge, it provides useful information on the implication of the reuse of alum sludge as adsorbent for P removal when the alum sludge is stored over a long time; (2) from the engineering point of view, the unchanged adsorption capacity is crucial in ensuring a sustainable pathway for the reuse of the alum sludge in environmental engineering applications.

Acknowledgements

References

[1] D. Jenkins, J.F. Ferguson, A.B. Menar, Chemical processes for phosphate removal, Water Res. 5 (7) (1971) 369–389.
[2] M. Razali, Y.Q. Zhao, M. Bruen, Effectiveness of a drinking-water treatment sludge in removing different phosphorus species from aqueous solution, Sep. Purif. Technol. 55 (3) (2007) 300–306.
[3] J. DeWolfe, Water Residuals to Reduce Soil Phosphorus, IWA Publishing, London, UK, 2006.
[4] Y. Yang, D. Tomlinson, S. Kennedy, Y.Q. Zhao, Dewatered alum sludge: a potential adsorbent for phosphorus removal, Water Sci. Technol. 54 (5) (2006) 207–213.
[5] Y. Yang, Y.Q. Zhao, A.O. Babatunde, L. Wang, Y.X. Ren, Y. Han, Characteristics and mechanisms of phosphate adsorption on dewatered alum sludge, Sep. Purif. Technol. 51 (2) (2006) 193–200.
[6] K.C. Makris, W.G. Harris, G.A. O'Connor, H. El-Shall, Long-term phosphorus effects on evolving physicochemical properties of iron and aluminum hydroxides, J. Colloid Interface Sci. 287 (2) (2005) 552–560.
[7] J.G. Kim, J.H. Kim, H. Moon, C. Chon, J.S. Ahn, Removal capacity of water plant alum sludge for phosphorus in aqueous solution, Chem. Speciation Bioavailability 14 (2002) 67–73.
[8] S.H. Huang, B. Chiswell, Phosphate removal from wastewater using spent alum sludge, Water Sci. Technol. 42 (3–4) (2000) 295–300.
[9] H. Roques, L. Nugroho-Jeudy, A. Lebugle, Phosphorus removal from wastewater by half-burned dolomite, Water Res. 25 (8) (1991) 959–965.
[10] S. Tanada, M. Kabayama, N. Kawasaki, T. Sakiyama, T. Nakamura, M. Araki, T. Tamura, Removal of phosphate by aluminum oxide hydroxide, J. Colloid Interface Sci. 257 (1) (2003) 135–140.
[11] H. Stefan, Mechanisms of phosphorus stabilization in the soil environment: A molecular scale evaluation. Ph.D. dissertation, University of Delaware, Newark, Delaware, USA, 2003.
[12] K. Okada, T. Nagashima, Y. Kameshima, A. Yasumori, T. Tsukada, Relationship between formation conditions, properties and crystallite size of boehmite, J. Colloid Interface Sci. 253 (2) (2002) 308–314.
[13] U. Schwertmann, J. Friedl, H. Stanjek, From Fe (III) ions to ferrihydrite and then to hematite, J. Colloid Interface Sci. 209 (1) (1999) 215–223.
[14] J. Berkowitz, M.A. Anderson, C. Amrhein, Influence of aging on phosphorus sorption to alum floc in lake water, Water Res. 40 (5) (2006) 911–916.
[15] J. Berkowitz, M.A. Anderson, R. Graham, Laboratory investigation of aluminum solubility and solid-phase properties following alum treatment of lake waters, Water Res. 39 (16) (2005) 3918–3928.
[16] J.T. Sims, B.G. Ellis, Changes in phosphorous sorption associated with aging of aluminum hydroxide suspensions, Soil Sci. Soc. Am. J. 47 (5) (1983) 912–916.
[17] K.C. Makris, Long-term stability of sorbed phosphorus by drinking water treatment residuals: Mechanisms and implications, Ph.D. dissertation, University of Florida, Gainesville, Florida, USA, 2004.
[18] APHA, AWWA, WEF, Standard Methods for the Examination of Water and Wastewater 18th ed., Washington, DC, USA, 1992.
[19] G. Tchobanoglous, F.L. Burton, H.D. Stensel, Wastewater Engineering: Treatment and Reuse, fourth ed., McGraw-Hill, London, UK, 2003.
[20] S. Brunauer, P.H. Emmett, E. Teller, Adsorption of gases in multimolecular layers, J. Am. Chem. Soc. 60 (2) (1938) 309–319.

[21] C. Pierce, Computation of pore sizes from physical adsorption data, J. Phys. Chem. 57 (2) (1953) 149–152.
[22] W.D. Harkins, G. Jura, Surfaces of solids. XIII. A vapor adsorption method for the determination of the area of a solid without the assumption of a molecular area, and the areas occupied by nitrogen and other molecules on the surface of a solid, J. Am. Chem. Soc. 66 (8) (1944) 1366–1373.
[23] R.S. Mikhail, S. Brunauer, E.E. Bodor, Investigations of a complete pore structure analysis. I. Analysis of micropores, J. Colloid Interface Sci. 26 (1) (1968) 45–53.
[24] B.C. Lippens, J.H. de Boer, Studies on pore systems in catalysts. V. The t method, J. Catal. 4 (3) (1965) 319–323.
[25] B.C. Lippens, B.G. Linsen, J.H. de Boer, Studies on pore systems in catalysts. I. The adsorption of nitrogen: apparatus and calculation, J. Catal. 3 (1) (1964) 32–37.
[26] J.R. Ferraro, Low-Frequency Vibrations of Inorganic and Coordination Compounds, Plenum Press, New York, USA, 1971.
[27] J.H. van der Maas, Basic Infrared Spectroscopy, second ed., Heyden & Son Ltd., London, UK, 1972.
[28] R.A. Weismiller, J.L. Ahlrichs, J.L. White, Infrared studies of hydroxy-aluminum interlayer material, Soil Sci. Soc. Am. Proc. 31 (1967) 459–463.
[29] R.D. Harter, J.L. Ahlrichs, Determination of clay surface acidity by infrared spectroscopy, Soil Sci. Soc. Am. Proc. 31 (1967) 30–33.
[30] M. Schnitzer, S.I.M. Skinner, The carbonyl group in a soil organic matter preparation, Soil Sci. Soc. Am. Proc. 29 (1965) 400–405.
[31] S. Brunauer, L.S. Deming, W.E. Deming, E. Teller, On a theory of the van der waals adsorption of gases, J. Am. Chem. Soc. 62 (7) (1940) 1723–1732.
[32] D.A. Georgantas, H.P. Grigoropoulou, Orthophosphate and metaphosphate ion removal from aqueous solution using alum and aluminum hydroxide, J. Colloid Interface Sci. 315 (1) (2007) 70–79.
[33] J.D. Hem, C.E. Roberson, Form and stability of aluminum hydroxide complexes in dilute solution, Chemistry of aluminum in natural water, Geological survey water-supply paper, 1827-A, United States Government Printing office, Washington, USA, 1967.
[34] S. Agyin-Birikorang, G.A. O'Connor, Lability of drinking water treatment residuals (WTR) immobilized phosphorus: aging and pH effects, J. Environ. Qual. 36 (2007) 1076–1085.
[35] W. Stumm, J.J. Morgan, Aquatic Chemistry: Chemical equilibria and Rate in Natural Waters, third ed., A Wiley-interscience Publication, John Wiley & Sons, New York, USA, 1996.
[36] K.F.N.K. Kwong, P.M. Huang, Influence of citric acid on the hydrolytic reactions of aluminum, Soil Sci. Soc. Am. J. 41 (1977) 692–697.
[37] P.H. Hsu, Formation of gibbsite from aging hydroxy-aluminum solutions, Soil Sci. Soc. Am. Proc. 30 (1966) 173–176.
[38] K.F.N.K. Kwong, P.M. Huang, Sorption of phosphate by hydrolytic reaction products of aluminium, Nature 271 (1978) 336–338.
[39] S.J. Gregg, K.S.W. Sing, Adsorption Surface Area and Porosity, Academic Press, New York, USA, 1982.
[40] R.S. Mikhail, S. Brunauer, E.E. Bodor, Investigations of a complete pore structure analysis. II. Analysis of four silica gels, J. Colloid Interface Sci. 26 (1) (1968) 54–61.
[41] C.J. Gommes, S. Blacher, J.P. Pirard, Nitrogen adsorption on silica xerogels or the odd look of a t plot, Langmuir 21 (5) (2005) 1703–1705.